step, the samples were implanted with magnesium ions using the MEVVA type TITAN implanter with unseparated ion beam, described in detail elsewhere. Ions were implanted at acceleration voltages between 20 to 67 kV which, at the average ionization multiplicity of magnesium ions equal to about 1.5, correspond to energies of about 30 to 100 keV, respectively. The implantation processes were carried out up to three ion fluences of $5x10^{17}$, $7x10^{17}$ and $1x10^{18}$ cm^{-2}. In the second step, the three HIPPB argon pulses were applied to melt the top layer of the Mg-B system. The plasma pulses were generated in a rod plasma injector (IBIS) type of accelerator described elsewhere. In the present experiments, the energy density of plasma were in the range of 0.8-3 J/cm^2. Pulse duration in the μs range corresponds to irradiance in the MW/cm^2 range. Scanning electron microscopy (SEM) was used to examine the changes of processed sample morphology with magnification ranging from 100 to 5000 times.

In order to get insight into the composition of the processed layer, the selected samples were subjected to the Rutheford backscattering (RBS) technique. The spectra were recorded using 1.7 MeV He^+ ion beam at normal incident to the sample. The backscattered particles were detected at an angle of 170° using a Si(Li) detector with the 15 keV energy resolution. The RBS spectra were fitted using a RUMP computer code.

In order to detect superconducting state of processed material three methods were used: magnetic measurements, magnetically modulated microwave absorption (MMMA) and four probe electric conductivity measurements.

The results of the sample characterization can be summarized as follows: Even as low pulse energy density, as 0.78 J/cm^2, is sufficient to melt the near surface layer of the substrate. After pulse treatment, the surface becomes relatively smooth, the edges of the craters (created as a result of chipping during surface polishing) are rounded. At higher energy densities, the morphology becomes rich of topographical features and the microcracks are also clearly visible. In spite of poor morphology, unexpectedly the sample treated with pulses of average energy density of 2.38 J/cm^2 appeared to be the best with respect to superconductive properties. The measured retained fluence in the as-implanted sample equal to $7x10^{17}$ cm^{-2} and decreases down to $6.4x10^{17}$ cm^{-2} after plasma pulses. RBS spectra exhibit that both process steps, especially pulse plasma treatment introduce excessive amount oxygen. The depth distribution profiles of magnesium atoms extracted from the spectra shows that. The depth distribution profiles of magnesium atoms extracted from the RBS spectra show that after pulse treatment, the magnesium to boron concentration ratio is closest to the stoichiometry of MgB_2 at about 100 nm thick surface layer. MMMA signals *vs*. temperature and external magnetic field are almost one order of magnitude stronger than that in the previous (B→Mg) [2] case. The T_c for the best samples is slightly above 25 K. At this temperature, also a sharp drop of electric resistively was observed. In spite of the presence of the substantial amount of the superconducting phase as confirmed by MMMA and resistivity measurements, no full macroscopic percolation occurred. This may be due to the two main reasons:

- microcracks at the top layer caused by rapid solidification;
- excessive amount of oxygen in the system, which may form MgO films insulating the superconductive regions.

Further experiments will be aimed at reduction of these two flaws.

References

[1]. Nagamats J., Nakagawa N., Muranaka T., Zenitani Y., Akimitsu J.: Nature, 410, 63-64 (2001).

[2]. Piekoszewski J., Kempiński W., Andrzejewski B., Trybuła Z., Piekara-Sady L., Kaszyński J., Stankowski J., Werner Z., Richter E., Prokert F., Stanisławski J., Barlak M.: Vacuum, 78, 123-129 (2005).

STRUCTURAL AND TRIBOLOGICAL PROPERTIES OF CARBON STEELS MODIFIED BY PLASMA PULSES

Bożena Sartowska[1/], Jerzy Piekoszewski[1,2/], Lech Waliś[1/], Jan Senatorski[3/], Jacek Stanisławski[2/], Lech Nowicki[2/], Renata Ratajczak[2/], Michał Kopcewicz[4/], Justyna Kalinowska[4/], Friedrich Prokert[5/], Marek Barlak[2/]

[1/] Institute of Nuclear Chemistry and Technology, Warszawa, Poland

[2/] The Andrzej Sołtan Institute for Nuclear Studies, Świerk, Poland

[3/] Institute of Precision Mechanics, Warszawa, Poland

[4/] Institute of Electronic Materials Technology, Warszawa, Poland

[5/] Institut für Ionenstrahlphysik und Materialforschung, Forschungszentrum Rossendorf e.V., Dresden, Germany

When steel is exposed to nitrogen incorporation at elevated temperature by such techniques as ion implantation, plasma immersion ion implantation (PI^3) and plasma nitriding, several nitrides are formed depending on the process conditions. Among all phases formed in this way an expanded austenite attracts a special interest of many authors [1-4]. Nitrogen expanded austenite (γ_N,) and carbon ex-

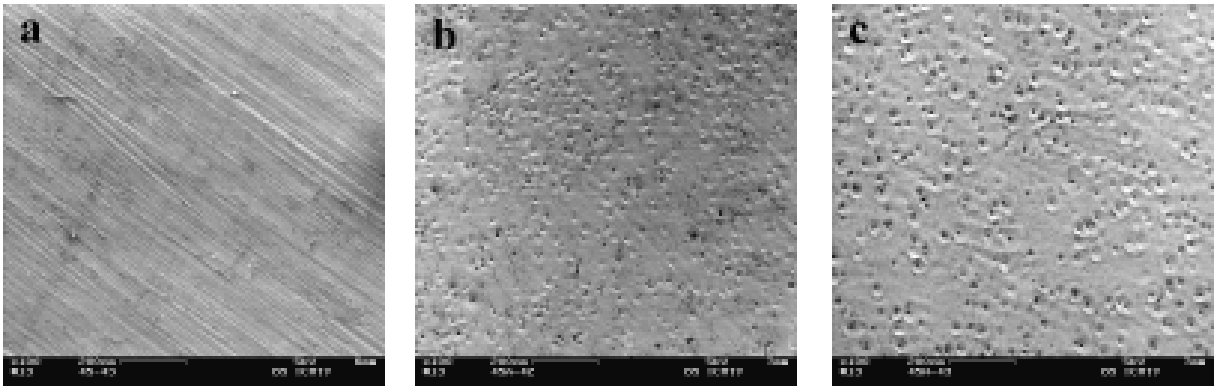

Fig.1. Surface morphology of steel 45: (a) untreated, modified with (b) argon and (c) nitrogen intense pulsed plasma beams.

panded austenite (γ_C) combine high hardness, good wear and corrosion resistance in austenitic stainless steels.

If the process of transient melting and recrystallization of the near surface layer of the substrate is applied, then the γ_N can be formed even in pure iron [5]. The expanded austenite is an interstitial solution of nitrogen or carbon where the nitrogen or carbon atoms are in octahedral interstitial sites in the fcc (face centered cubic) crystal lattice of the austenite. Increase of fcc structure lattice parameter depends on the contents of interstitials. Nitrogen atoms having the smaller radius compared to carbon, but cause a higher dilatation being dissolved in the fcc lattice. Nitrogen atoms in austenite increase the concentration of free electrons, *i.e.* enhance the metallic component of atomic interactions. Carbon atoms are expected to contribute to the localized electrons, *i.e.* to enhance covalent bonds [6].

Carbon steels with different concentration of carbon and heat treated according to the standard procedures were used: Armco-iron, steels 20, 45, 65 and N9. The samples were irradiated with five intense (about 5 J/cm^2), short (μs range) argon or nitrogen plasma pulses generated in a rod plasma injector (RPI) type of plasma generator.

Samples were characterized by the following methods: nuclear reaction analysis (NRA) $^{14}N(d,\alpha)^{12}C$, scanning electron microscopy (SEM), conversion electron Mössbauer spectroscopy (CEMS), X-ray diffraction analysis (GXRD) with grazing incidence angle between 0.5 and 2° and Amsler wear tests.

Of all nitrogen plasma treated samples only those were selected in which the retained dose of nitrogen is equal to $1.2x10^{17}\pm2x10^{16}$ N/cm^2.

SEM observations shown that the morphology of the pulse treated samples, both argon and nitrogen plasma are identical. The craters and droplets are uniformly distributed over the surface, which is typical of melted and rapidly recrystallized top layers (Fig.1). The thickness of the modified layers is in the range of 1.2-1.6 μm.

Table. Content of phases [vol.%] identified at the surface layer of initial and modified carbon steels.

Material		Argon				Nitrogen				
Steel	%C	α-Fe	α'	γ_0	γ_C	α-Fe	γ_0	γ_C	γ_N	ε-Fe_3N
Armco	0.018	100				68.04	11.85	1.35	11.06	7.71
20	0.28	78.1	12.58	6.22	3.1	35.24	33.5	11.39	14.99	4.87
45	0.52	71.33	13.19	10.56	4.91	27.76	39.12	8.87	20.34	3.91
65	0.63	54.48	10.22	22.89	12.41	27.01	35.23	10.54	17.85	9.37
N9	0.93	47.91	6.61	27.83	17.65	26.6	36.73	17.25	13.67	5.64

Combined computer fitting of the CEMS spectra taken on full and reduced velocity scale enabled us to determine the contribution of each of the identified phase (Table). The general observation is that nitrogen is much more efficient than argon in ausenitization of carbon steel. For example, 15.5 vol.% of fcc phases was detected in steel 45 (containing 2.2 at.% C) treated with argon pulses, whereas 60% of fcc phases were detected in steel 20 which after nitrogen plasma treatment contains 1.0 at.% C and 1.5 at.% N.

Figure 2 shows the GXRD patterns taken at the incidence angle between 0.5 and 2° for martensitic α'-Fe: initial, argon and nitrogen pulse plasma treated. Only reflections characteristic of α'-Fe are observable in untreated sample. After argon pulses treatment, two additional γ reflections: at 2θ≈50.5° and 74.4° are clearly seen. Unfortunately, at such small content of carbon it is impossible to resolve γ into γ_0 and γ_C, as it was possible with CEMS. After nitrogen plasma treatment, the γ reflections are much stronger than for argon ones although resolution of γ into γ_0, γ_C and γ_N is also impossible. From the shift of γ(111) toward the smaller 2θ, it was estimated that lattice expansion of fcc by about 0.8% occurs. Comparing the intensities of α'(111) and γ(111) in the range of 2θ=43-46° one can see that for incident angle 2° the α'(111) peak is stronger that that of γ(111), and for lower angles the situation is reverse. This

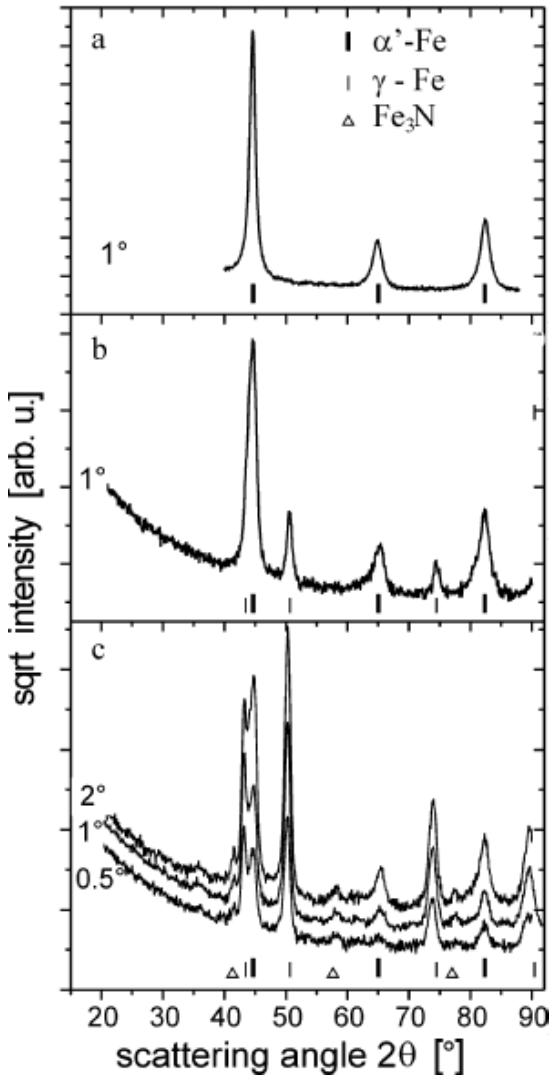

Fig.2. GXRD spectra for steel 65: (a) initial modified with (b) argon and (c) nitrogen intense pulsed plasma beams.

suggests that the top layer is composed of a mixture of this two phases. GXRD pattern shows also the presence of ε-Fe_3N by peaks at 41.2, 57.8 and 77.5°. In general, GXRD confirms at least qualitatively the results derived from the CEMS data.

Figure 3 shows the results of the linear wear measurements on initial, argon and nitrogen plasma treated samples of carbon steels. The wear was lower for all the modified samples as compare with the initial material. Substantial improvement of wear for argon and nitrogen treated samples is observed only for lower carbon steels. Results obtained for high carbon steel – N9 – show a significantly lower linear wear than for low carbon steels. Greater improvement of tribological properties occurs for nitrogen than for argon treatment, which can be explained by the presence of nitrogen phases (γ_N and ε). SEM observations of the wear tracks morphology show the parallel grooves and scratches in the direction of sliding and allowed us to state that the microcutting together with the plastic deformation was the main wear mechanism existing here.

In contrast to γ'-Fe_4N which yields the most wear resistant surfaces, the ε-Fe_3N is not identified as a phase that improves tribological properties of nitrided steels [1,7]. No γ'-phase was detected in our samples, therefore improvement of wear resistant in our case we ascribe as being due mainly to the presence of γ_N phase.

In conclusions: The nitrogen expanded austenite – γ_N phase was detected in the near-surface region of Armco and carbon steels in the case of

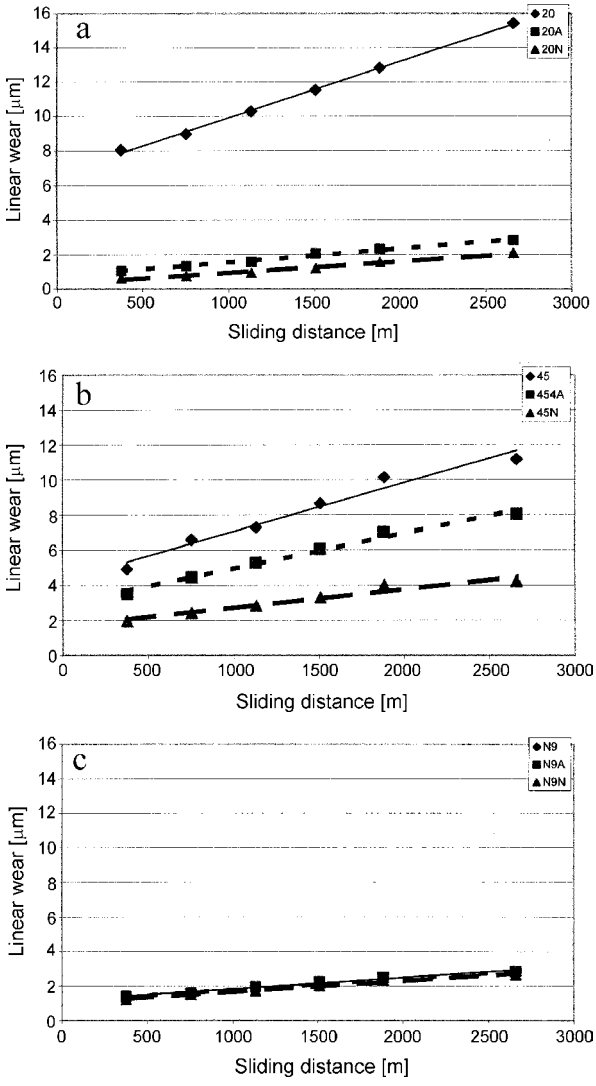

Fig.3. Linear wear of untreated and modified with intense plasma pulses: steel 20 (a), steel 45 (b) and steel N9 (c).

nitrogen plasma modification. Significant increase of the hardness and tribological properties of modified surfaces occurs for nitrogen treatment, which can be explained by the presence of γ_N phase.

References

[1]. Williamson D. L., Oztruk O., Glick S., Wie R., Wilbur P.J.: Nucl. Instrum. Meth. Phys. Res. B, 59/60, 737-741 (1991).

[2]. Collins G.A., Hutchings R., Short K.T. , Tendys J., Li X., Samandi M.: Surf. Coat. Technol., 74-7, 417-424 (1995).

[3]. Jirásková Y., Schneeweiss O., Perina V., Blawert C., Mordike B.L.: Phase composition of steel surfaces after plasma immersion ion implantation. In: Mössbauer spectroscopy in materials science. Kluwer Academic Publishers, Amsterdam 1999, pp.173-182.

[4]. Günzel R., Betzl M., Alphonsa I., Ganguly B., John P.I., Mukherjee S.: Surf. Coat. Technol., 112, 307-309 (1999).
[5]. Sartowska B., Piekoszewski J., Waliś L., Szymczyk W., Stanisławski J., Nowicki L., Ratajczak R., Kopcewicz M., Kalinowska J., Barcz A., Prokert F.: Vacuum, 78, 181-186 (2005).
[6]. Gavriljuk V.G., Berns H.: High nitrogen steels. Structure, properties, manufacture, applications. Springer-Verlag, Berlin Heilderberg 1999, 376 p.
[7]. Williamson D.L., Wang L., Wie R., Wilbur P.J.: Mater. Lett., 9, 9, 302-308 (1990).

UV IRRADIATION OF TRACK MEMBRANES AS A METHOD FOR OBTAINING THE NECESSARY VALUE OF BRITTLENESS FOR GOOD FRACTURES OF SAMPLES FOR SEM OBSERVATIONS

Bożena Sartowska, Oleg Orelovitch[1/], Andrzej Nowicki

[1/] Flerov Laboratory of Nuclear Reactions, Joint Institute for Nuclear Research, Dubna, Russia

Synthesis of nano- and microstructures of materials inside the pores of specific template-track membranes can be used to obtain nano- and microwires or nano- and microtubes [1]. It is important for these applications to know the inner geometry of the pores like sizes, shape and surface morphology [2,3]. Scanning electron microscopy technique (SEM) was used for this kind of membrane characterisation. The proper preparation of samples for SEM observations is very important in order to prevent destruction of the structure of membrane during the fracture preparation. The breaking membranes samples at the liquid nitrogen temperature (77 K) did not allow us to obtain undistorted cross-section. The use of other methods of sample preparation as electron, gamma rays or UV irradiation allows us to make them more brittle [4-6]. The preliminary results of tensile measurements of membranes after UV irradiation are presented here.

Poly(ethylene terephthalate) (PET) membrane 10 μm thick with pore diameter 1.0 μm were prepared at the Joint Institute for Nuclear Research (Dubna, Russia) using the standard procedure [3]. Then, the samples were irradiated with UV light with energy flux 2.8 W/cm^2 during different periods of time. The tensile measurements of the initial and irradiated materials were carried out using a tensile machine Instron 5565 (Instron Co., England) in the Institute of Nuclear Chemistry and Technology. Membranes surface and fracture observations were made using SEMs: JSM 840 (Jeol, Japan), DSM 942 (Zeiss, Germany) and LEO 1530 GEMINI (Zeiss, Germany) with low accelerating.

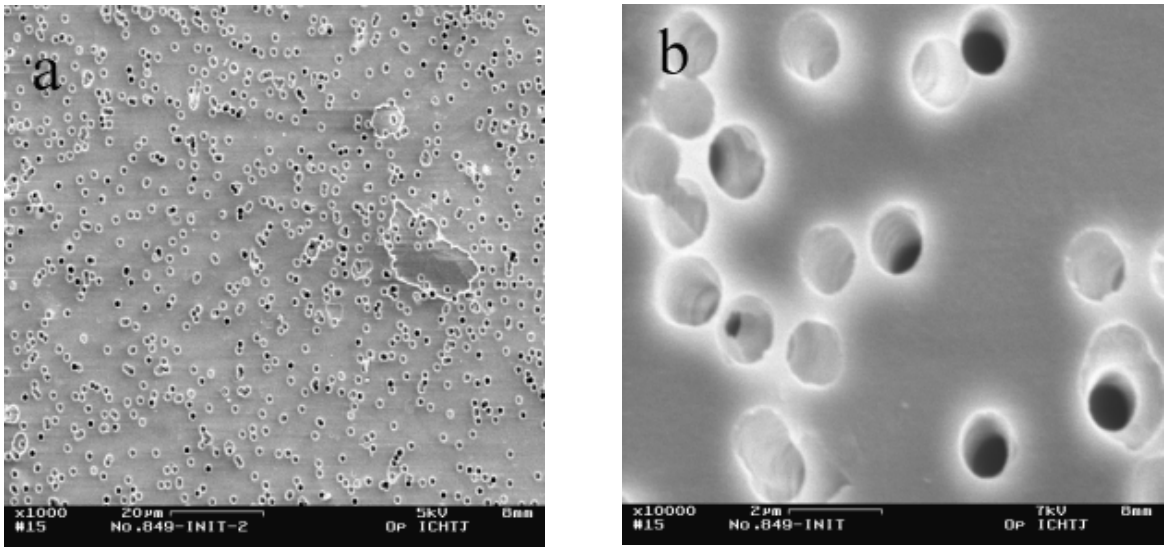

Fig.1. Surface morphology of PET investigated membrane: a) x1000 magnification and b) x10 000 magnification.

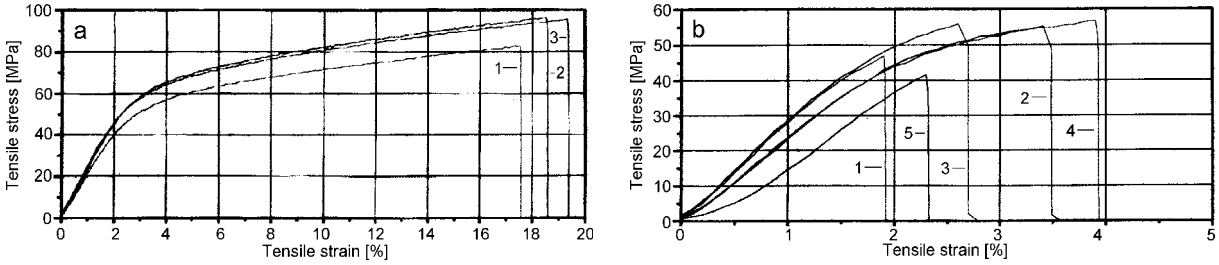

Fig.2. Samples of tensile measurements results of PET membrane: a) initial and b) after 52 h UV irradiation.